Measuring orbitals and bonding in atoms, molecules, and solids

Maarten Vos[a] and Ian McCarthy
Electronic Structure of Materials Centre, Flinders University of South Australia, GPO Box 2100, Adelaide, S.A., 5001, Australia

(Received 20 May 1996; accepted 9 December 1996)

The cloud of negative charge that determines the relative positions of the nuclei in a molecule or solid can be understood in terms of the motion of the electrons that form the cloud. Usually one pictures the charge cloud as a distribution in coordinate space. One can equally well picture it as a distribution of velocities, i.e., in momentum space. The probability that an electron has a certain energy–momentum combination is called the energy–momentum density. It is directly measured by electron-momentum spectroscopy. The results of this technique provide the most direct experimental documentation of simple ideas of orbitals and bonding, thus opening a fresh and comprehensive perspective on electronic structure. We show how measurement of the motion of electrons in solids can help us understand the bonding of atoms in molecules and solids. We give examples of a free-electron metal and an ionic insulator.

I. INTRODUCTION

A major aim of physics is to obtain direct measurements of properties closely related to the electronic wave functions of atoms, molecules and solids. This goal has been somewhat elusive. Most techniques measure properties that are related in a rather indirect way to the wave function; for example, absorption and emission spectroscopies measure the differences between energy levels. The resistivity of a metal is another indirect property.

The technique that measures quantities most closely related to the wave function is electron-momentum spectroscopy (EMS).[1] Here the kinetic energies and momenta of an incident electron and two outgoing electrons, detected in time coincidence, are observed and recorded for a large number of events. For each event the sum of the kinetic energies and momenta of the two outgoing electrons is different from the kinetic energy and momentum of the incident electron. The energy difference is the binding energy of the target electron. For high enough energies of the external electrons, the momentum difference is equal to the momentum of the target electron just before the collision. The experiment therefore estimates, from the number of target electrons in each small energy–momentum range, the probability of finding an electron in that range. This is the energy–momentum density of target electrons. The experimental criterion for high enough energy is that the measured energy–momentum density should not change if the energy of the incident electron is increased.

The relationship of the energy–momentum density to the ground state wave function of an electronic system is easily understood in terms of the independent-particle model, in which the motion of each electron is determined by a one-electron function, called an orbital. The orbital is the solution of a Schrödinger equation for the motion of an electron in an electrostatic potential determined by the nuclei and the self-consistent motion of all the electrons. Each orbital is often calculated as a function of the position of the electron, but it is mathematically equivalent to the orbital represented as a function of the electron momentum. Each function is the Dirac–Fourier transform of the other. Each orbital represents an electron with a particular eigenvalue of energy. Its absolute square gives the probability of finding the electron in a particular small range of momentum. Hence, a calculation of all the orbitals gives the density of the orbitals per unit energy interval and thus the energy–momentum density which we compare with experiment.

Although both coordinate and momentum representations contain identical information, we are more accustomed to visualizing things in coordinate space. We therefore first describe atomic orbitals in momentum space, form an idea of how the orbitals form a chemical bond, and show how the hydrogen-molecule bond can be observed by EMS.

To illustrate the transition from a molecule to a crystalline solid we show a one-dimensional model in which, for a large number of atoms, each orbital is associated with a unique value of momentum. The relationship of the momentum to the energy eigenvalue of the orbital is the dispersion relation for the resulting band of one-electron states, which becomes essentially continuous in the limit of a large crystal. We use the insights developed here to understand the EMS results for two completely different solids, metallic aluminum and aluminum oxide, which is an ionic insulator. In this way we develop a unified understanding of atomic, molecular and solid-state physics, based on EMS.

Two other techniques determine momentum information about electrons in materials. Compton scattering[2,3] determines energy-summed and partially momentum-integrated probabilities. Angle-resolved photoelectron spectroscopy[4] determines the band dispersion relations in terms of energy and crystal momentum for electrons in a single crystal with a flat surface. Crystal momentum is essentially a set of quantum numbers characterizing the orbital at a particular energy. It is a property of the crystal lattice. EMS determines the density of the electrons as a function of their energy and real momentum, irrespective of crystal structure. It applies to gaseous, amorphous or polycrystalline materials as well as to single crystals.

For a more technical description of EMS as applied to atoms and molecules we refer to McCarthy and Weigold.[1] For applications to solids see Vos and McCarthy[5] and Dennison and Ritter.[6] Here, it is necessary to have target thicknesses no greater than about 100 Å, because the external electrons must be transmitted through the target. Recently it has become possible to study larger organic molecules with this technique as well. This application has been described by Zheng *et al.*[7]

II. WHAT IS MEASURED BY EMS?

The experiment uses a beam of electrons of known kinetic energy E_0 and known direction. Its momentum $\mathbf{k}_0$ is therefore known. The beam is incident on a target consisting of atoms, molecules, or a solid film. The incident electron knocks a second electron out of the target. Both the electron from the incident beam and the knocked-out target electron are detected after the collision. Their kinetic energies and momenta, E_f and $\mathbf{k}_f$ for the faster one and E_s and $\mathbf{k}_s$ for the slower one, are observed.

One can deduce the binding energy ϵ and momentum $\mathbf{q}$ of the target electron from the conservation laws, assuming that the energies and momenta of the external electrons depend only on the motion of the two colliding electrons immediately before and after the collision. This assumption is discussed below:

$$\epsilon = E_0 - E_s - E_f \tag{1}$$

and

$$\mathbf{q} = \mathbf{k}_s + \mathbf{k}_f - \mathbf{k}_0 . \tag{2}$$

In the independent-particle model, the probability that one measures a certain binding-energy–momentum combination is proportional to the absolute square of the momentum-space orbital of the target electron $|\phi_\epsilon(\mathbf{q})|^2$. The momentum-space orbital is related to the coordinate-space orbital $\psi_\epsilon(\mathbf{r})$ by the Dirac–Fourier transformation,

$$\phi_\epsilon(\mathbf{q}) \equiv \langle \mathbf{q} | \phi_\epsilon \rangle = (2\pi)^{-3/2} \int d^3r \, \exp(-i\mathbf{q}\cdot\mathbf{r}) \psi_\epsilon(\mathbf{r}). \tag{3}$$

Thus both contain the same information. However what is measured is the absolute square of the momentum-space orbital, so the phase information is lost. One cannot obtain $|\psi_\epsilon(\mathbf{r})|^2$ from $|\phi_\epsilon(\mathbf{q})|^2$ or vice versa.

In the case of atoms or molecules the energy ϵ of the orbital can often be resolved, so that we measure the momentum density $|\phi_\epsilon(\mathbf{q})|^2$. For a large system such as a solid there are many orbitals within the resolvable energy interval. What we then measure is the energy–momentum density, i.e., the average for the energy interval of all the momentum densities.

Equation (2) assumes that momentum changes to the external electrons are due only to the elementary electron–electron collision and not to effects of their interaction with the remainder of the target system. Such effects are characterized by the generic term ''distortion,'' since they distort our knowledge of $\mathbf{q}$. Distortion effects are small if each external electron has a high enough energy. There is an experimental criterion for the energy. If the target energy–momentum density deduced from an experiment does not change when the external energies are substantially increased, then they are high enough. The beauty of the technique is that the energy and momentum of the target electron are determined by subtraction, so that arbitrarily high external energies, consistent with experimental feasibility, can be used. Therefore the high-energy criterion can be satisfied independently of the target energy–momentum range to be observed. The experiment is set up to scan a range of energy and momentum, the rate of coincidence counts in particular small energy–momentum intervals giving an energy–momentum density profile.

From the experimental point of view, the main challenge is the detection of the slow and fast electrons in coincidence so as to determine which pairs of electrons originate from the same collision. Coincidence experiments have been notoriously difficult because of slow count rates. The first EMS experiment was on solid carbon. Each detector was tuned to a single energy and momentum, with an energy resolution of 90 eV, and the count rate was of the order of one count per minute.[8] Nowadays, we can get count rates three orders of magnitude larger by the use of detectors that measure simultaneously a range of energies and a range of momenta. Energy resolution is approximately 1 eV, which is good enough to distinguish electronic states in most cases. Vibrational and/or rotational bands built on the electronic states are not resolved and do not affect the energy–momentum profiles.[1] Momentum resolution is approximately 0.1 a.u.

Throughout the article we use Hartree atomic units (a.u.), for which $e = m = \hbar = 1$, where m is the electron mass. The atomic unit of length is the Bohr radius of the hydrogen atom, $a_0 = 0.529$ Å. The atomic unit of momentum is $\hbar/a_0$, which is 1.89 Å^{-1}. In atomic units, momenta and reciprocal lengths (for example, wave numbers) have the same numerical values. For energy we use the laboratory unit, electron volt (eV); 1 a.u. of energy corresponds to 27.2 eV.

A difficulty of the technique in the case of solid targets is that, if one wants to measure the complete energy–momentum density profile down to zero momentum, one can do it only if one uses transmission experiments through thin films. For Eqs. (1) and (2) to apply, it is necessary that no additional collisions occur along any of the three trajectories of the external electrons. Due to the small mean free path of electrons in the appropriate energy range 1–20 keV, it is necessary for the films to be very thin (roughly 100 Å). Only for such thicknesses will the desired electronic structure information not be obscured by distortion. A schematic drawing of the spectrometer for solid samples at Flinders University is given in Fig. 1. For more details see Storer *et al.*[9]

To give a more-detailed description of what is measured, we need the probability amplitude for a reaction with a many-body target ground state 0 and a final electronic ion state I that is isolated by the binding-energy measurement. The probability, and hence the experimental count rate, is proportional to the absolute square of the amplitude, which is expressed as the matrix element of an operator T that governs the transition between the initial and final states of the colliding system,

$$F_{I0}(\mathbf{k}_0, \mathbf{k}_f, \mathbf{k}_s) = \langle \mathbf{k}_f \mathbf{k}_s I | T | 0 \mathbf{k}_0 \rangle. \tag{4}$$

The kinematic conditions of the experiment are chosen[1] so that the amplitude is essentially proportional to the quantity

$$\begin{aligned} \langle \mathbf{q} I | 0 \rangle &= \langle \mathbf{k}_f \mathbf{k}_s I | 0 \mathbf{k}_0 \rangle \\ &\equiv (2\pi)^{-3/2} \int d^3r_1 \cdots \int d^3r_N \\ &\quad \times \exp(-i\mathbf{q}\cdot\mathbf{r}_1) \Psi_I^*(\mathbf{r}_2, \ldots, \mathbf{r}_N) \Psi_0(\mathbf{r}_1, \ldots, \mathbf{r}_N), \end{aligned} \tag{5}$$

which we call the structure amplitude. The notation Ψ denotes a many-body wave function for the system indicated by the subscript. The electron coordinates are $\mathbf{r}_1, \ldots, \mathbf{r}_N$. The kinematic conditions are essentially the high-energy conditions described above and the approximation involved has the same experimental verification.

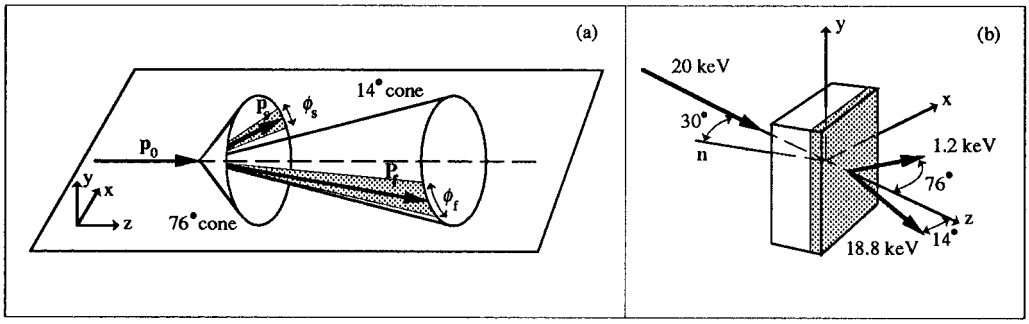

Fig. 1. In (a) we show the collision geometry of the experiment. Two analyzers detect the emerging particles over a range of angles. If two electrons are detected at the same time, they would originate from the same event. From the measured momenta and energies we can infer the binding energy and momentum of the target electron before the collision. In (b) we show the target geometry, and the approximate energies of the incident and detected electrons. Due to the short mean free path of the 1.2-keV electron, most information is obtained from the shaded part of the 100-Å-thick film.

In the independent-particle model the ion state I results from taking an electron from an orbital of the target, whose energy is ϵ. The structure amplitude is then

$$\langle \mathbf{q}I|0\rangle = \langle \mathbf{q}|\phi_\epsilon\rangle = \phi_\epsilon(\mathbf{q}), \tag{6}$$

and the count rate is proportional to $|\phi_\epsilon(\mathbf{q})|^2$.

A refinement is to consider the target ground state 0 in a full many-body representation and the ion state I as a linear combination of states formed by removing an electron from one orbital of an arbitrary target eigenstate. The coefficients in the linear combination for each ion eigenstate are found by diagonalizing both the target and ion Hamiltonians in a representation constructed from target orbitals. Only the one-hole states formed by removing an electron from an orbital of appropriate symmetry in the target ground state will have a finite projection on the ground state, since the target eigenstates are orthogonal. Each projection is a momentum-space orbital $\phi_\epsilon(\mathbf{q})$. To a good approximation, if the orbital set is well chosen, only one will contribute to the one-hole linear combination of orbitals. Thus many-body ion states are associated by the reaction with particular orbitals[1] and Eq. (6) still applies.

III. ATOMIC ORBITALS IN MOMENTUM SPACE

To get more of a feeling for the representation of the orbitals in momentum space, we show in Fig. 2 examples of the densities for orbitals of the hydrogen atom. As there is only one electron, it is possible to solve the Schrödinger equation exactly. We plot densities in coordinate space as well as momentum space. We do this for electrons in the ground state ($1s$ orbital), and the lowest two excited states ($2s$ and $2p$ orbitals). Let us stress that there are a lot of similarities between the orbitals in momentum and coordinate space. The symmetry properties of each orbital are identical in both representations; even the shapes are similar. One of the major differences is that those orbitals whose density is confined to a region close to the origin in coordinate space (e.g., the $1s$ orbital) extend far away from the origin in momentum space (and vice versa), as expected on the basis of the uncertainty principle.

More generally it turns out that the low-momentum part of $\phi_\epsilon(\mathbf{q})$ is related to the distant part of $\psi_\epsilon(\mathbf{r})$. This is intuitively clear if one realizes that near the nucleus the electron has little potential energy and a lot of kinetic energy, whereas far away the situation is reversed. Similarly, chemical bonding in molecules is due to the interference of atomic orbitals far from the nuclei and will show up as significant deviations from the atomic orbitals at small values of $\mathbf{q}$.

All the diagrams of Fig. 2 are the results of calculations. The only one of these that has been verified experimentally is the hydrogen $1s$ momentum density. This was done by Lohmann and Weigold[10,11] using EMS of hydrogen atoms made by dissociating molecular hydrogen by the application of a strong radio-frequency field. In Fig. 3 we compare the experimental momentum density with the absolute square of the analytic solution of the Schrödinger equation in momentum space. The agreement is excellent.

The $2s$, $2p$ and higher orbitals are not occupied for hydrogen in the ground state and hence we cannot measure them in EMS. However, one can measure analogous orbitals for heavier elements where they are occupied. Due to the larger nuclear charge these orbitals contract in coordinate space (and hence become more extended in momentum space) relative to the ones calculated for the hydrogen atom. There are corrections due to the influence of the other occupied orbitals. The many-electron problem of course requires numerical approximations. The self-consistent-field (SCF) approximation calculates an orbital in an electric field due to the nucleus (or nuclei for molecules and solids) and the self-consistent motion of the other electrons, taking account of the Pauli exclusion principle. There remains a general resemblance between the higher hydrogen orbitals and these atomic orbitals.

For the argon atom we show in Fig. 4 the momentum densities of the $3s$ and $3p$ levels, which are its outermost occupied levels, observed with the spectrometer used at Flinders for studying solids. Again the s density is spherically symmetric and has a maximum (both in coordinate and momentum space) at the origin. The density for a fully occupied p level (the sum of the absolute squares of p_x, p_y, and p_z densities) is again spherically symmetric. However, it still has a node at the origin. The small density measured at zero momentum is a consequence of the finite momentum resolution of the experiment, which is built into the corresponding calculation.

IV. THE CHEMICAL BOND IN MOMENTUM SPACE

The next step is to get some understanding of the chemical bond and how it affects the orbitals in momentum space. In

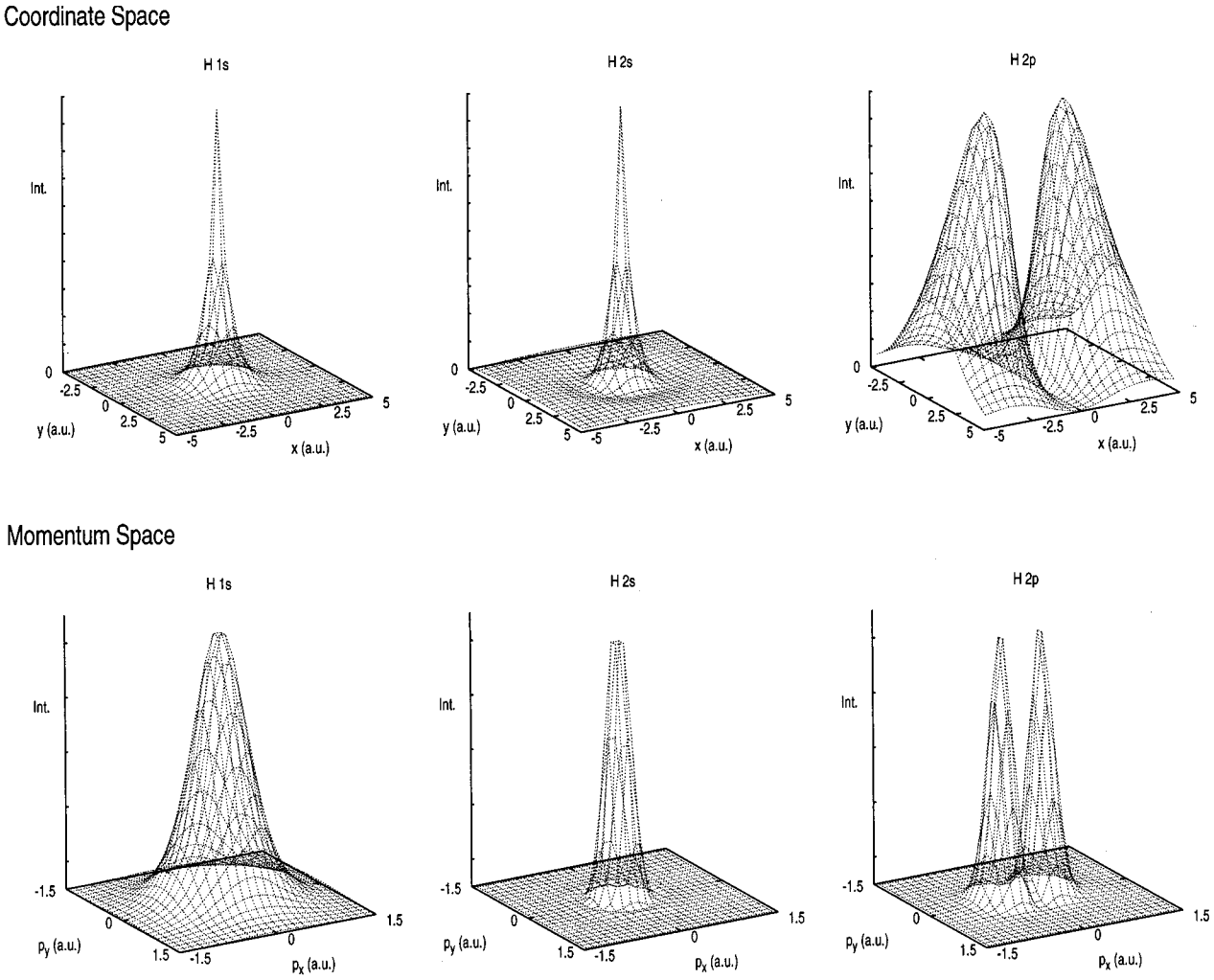

Fig. 2. Three-dimensional plots of the probability density $|\psi(x,y,0)|^2$ in coordinate space and the probability density $|\phi(p_x,p_y,0)|^2$ in momentum space are shown for the $1s$, $2s$, and $2p_y$ orbitals of the hydrogen atom. Note that in momentum and coordinate space the orbitals have the same symmetry. Also note that the more extended the orbital is in coordinate space, the more confined in momentum space. The node for the $2s$ orbital results in a density minimum which is visible as a circle centered at the origin in both the coordinate- and momentum-space pictures.

this context it is interesting to note an early discussion by Coulson,[12] who emphasized the potential of momentum information for studying chemical bonding. At that time partially momentum-integrated and energy-summed information on molecular momentum densities could be obtained from Compton scattering.[2,3]

The prototype for the discussion of the chemical bond is the hydrogen molecule. The distance between the nuclei in a hydrogen molecule is 1.4 a.u. (0.74 Å). This is considerably smaller than the spatial extension of two atomic hydrogen $1s$ orbitals (see Fig. 2), each of which has an rms charge radius of 1.73 a.u. The orbitals of two undisturbed hydrogen atoms at the molecular distance would therefore overlap.

The chemical bond is described by molecular orbitals that are SCF solutions of the molecular Schrödinger equation. The most stable solution is one that minimizes the total energy of the system. There are different types of molecular orbitals, each with a different symmetry property. In a simplified description we understand them in terms of linear combinations of atomic orbitals. For two identical atoms, indistinguishability of the electrons limits the possible combinations of atomic orbitals to two, one symmetric and one antisymmetric. The antisymmetric combination has a nodal plane equidistant from the nuclei. Nonidentical atoms result in analogous molecular orbitals, but the nodal surface in the analogue of the antisymmetric orbital is deformed and displaced. The electron density is the squared magnitude of the molecular orbital.

The key to understanding the energies of different types of molecular orbitals in the atomic-orbital picture, and therefore their bonding properties, is the density of negative charge resulting from the interference of the overlapping atomic orbitals. This is called the interference density.[13] The interference of s orbitals is constructive in the symmetric case, destructive in the antisymmetric case.

We first compare the symmetric combination of two $1s$ orbitals with two bare $1s$ orbitals at the molecular distance. Constructive interference results in charge density being redistributed from the region near the nuclei to the overlap region between the nuclei. The density changes are of two kinds.

First, the volume occupied by the electrons becomes larger and the density smoother. This results in a significant lowering of the kinetic energy, since lower absolute momenta re-

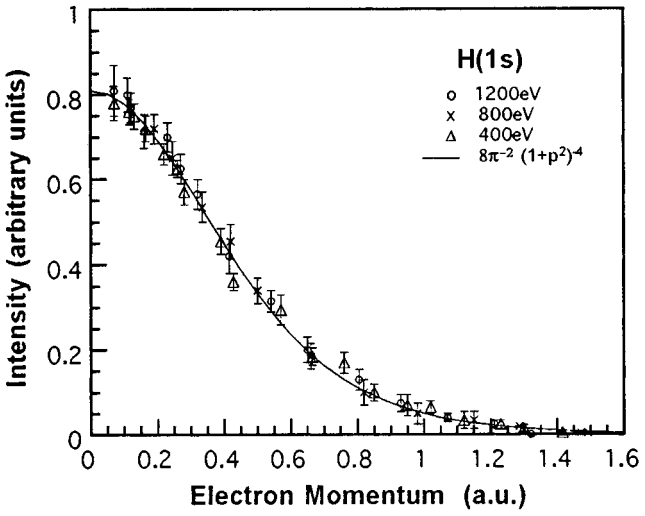

Fig. 3. The experimental measurement of $|\phi(\mathbf{q})|^2$ for the hydrogen atom. The experiment was done using three different energies of the incoming electrons, as indicated in the figure. All three experiments gave identical momentum densities. The exact solution of the Schrödinger equation (solid curve) fits the EMS data perfectly.

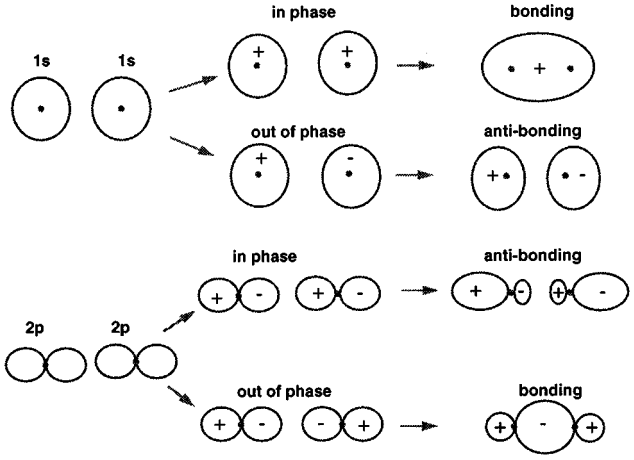

Fig. 5. The chemical bond derived from (a) *s* orbitals and (b) *p* orbitals. In the case of *s* orbitals the bonding molecular orbital is formed if the orbital on one atom is obtained from the orbital on the other atom by a simple translation. For the *p* orbitals the bonding orbital is formed if the orbital on one atom is obtained from the orbital on the other by a translation *and* multiplication by -1.

sult from larger volumes and smaller orbital gradients. We call this the overlap effect. Potential-energy changes in the overlap region are comparatively small.

The redistribution results in reduced density near each nucleus, causing the second effect which is called promotion. The reduced charge cloud is attracted to the nucleus more strongly so that the effective atomic orbital shrinks in space. We can model each effective atomic orbital by $\exp(-\zeta r)$.

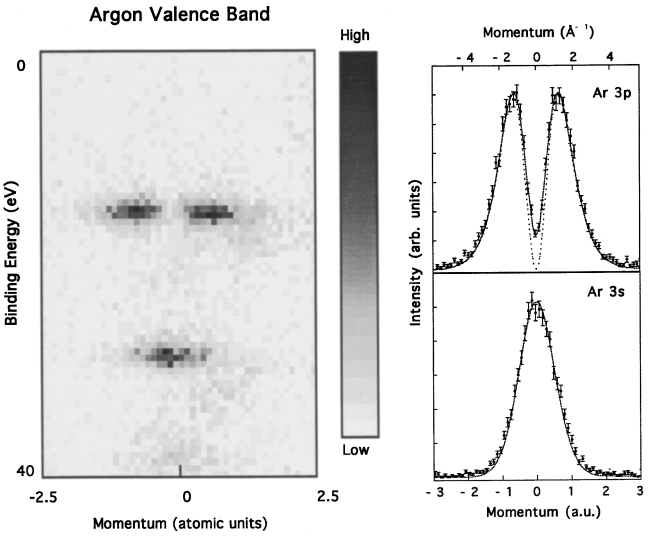

Fig. 4. The measured energy–momentum density of the valence levels of argon gas. On the left we show it as a greyscale plot. There is significant density for two different binding energies corresponding to the $3p$ and $3s$ orbitals. Their completely different nature is evident from the fact that the $3s$ electrons have maximum density at zero momentum, whereas the $3p$ electrons have minimum density at zero momentum (the density would be zero for perfect momentum resolution). In the right half we show a comparison of the measured momentum densities with ones obtained from SCF calculations (broken curves) and after convolution with the experimental momentum resolution (full curves).

For the hydrogen-molecule bond the decay constant ζ increases from 1 in the bare-atom case to 1.193 in the molecular case. The kinetic energy is considerably increased and the potential energy considerably decreased. These changes almost balance for the hydrogen molecule.

In comparison with two bare atoms at the molecular distance there is a net increase in kinetic energy due to the competing effects of promotion and the overlap region. This is outweighed by the decrease in potential energy due to promotion. The decisive effect is the decrease in kinetic energy in the overlap region, since the effects of promotion on the kinetic and potential energies almost cancel. The symmetric combination is a bonding orbital.

The energy arguments work exactly in reverse for the antisymmetric combination. Charge is taken from the overlap region and placed near the nuclei. The increased density gradient causes an increase in kinetic energy, which is decisive in the bonding consideration. The promotion effect is an expansion of the effective atomic orbitals, with the corresponding decay constant being smaller than for bare atoms. The antisymmetric combination is an antibonding orbital.

Bonding for *p* orbitals is different from that for *s* orbitals. A *p* orbital has lobes of opposite sign on opposite sides of the nucleus. Hence increased interference density in the overlap region, resulting in a bonding molecular orbital, is obtained by adding adjacent *p* orbitals with opposite signs. The antisymmetric combination is the bonding orbital. We show later that this difference results in different behavior of *s*- and *p*-derived electronic states in ionic solids (see Fig. 5).

There is another approach to the hydrogen molecule. As we have seen before, the highest momentum density is near the origin and corresponds to the part of the orbital in coordinate space that is far away from the nucleus. At large distances one electron experiences the attractive potential of two protons, rather close together and screened by the other electron. Near the origin the momentum-space orbital therefore resembles that of a $1s$ electron in a helium atom.

To what extent is the momentum profile influenced by the bonding? In Fig. 6 we show the absolute squares of calculated bonding and antibonding orbitals of the hydrogen mol-

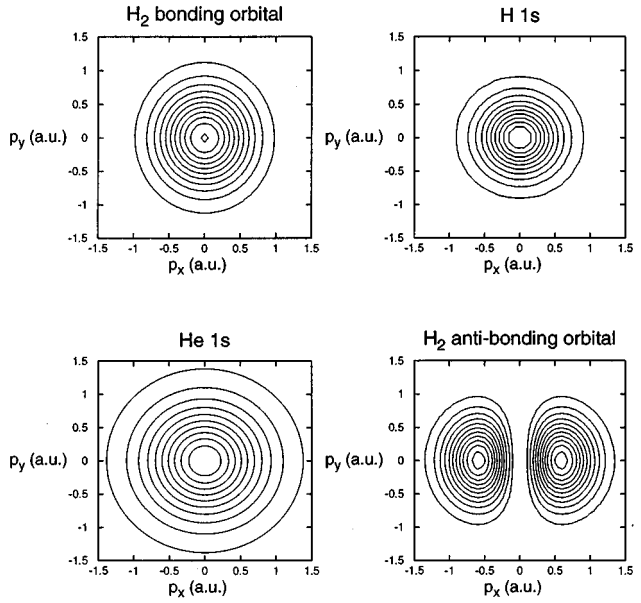

Fig. 6. Chemical bonding in momentum space. In the top panel we show the momentum density distribution of the bonding orbital for a hydrogen molecule oriented along the x axis. As the electrons become more delocalized along the x axis the distribution becomes narrower along the p_x axis. At large distances the electrons probe the attractive potential of two protons screened by one electron. The resulting momentum distribution for the bonding orbital is then between those of the 1s orbital of the hydrogen atom and the 1s orbital of helium. The antibonding orbital peaks at larger momentum values and thus has more kinetic energy.

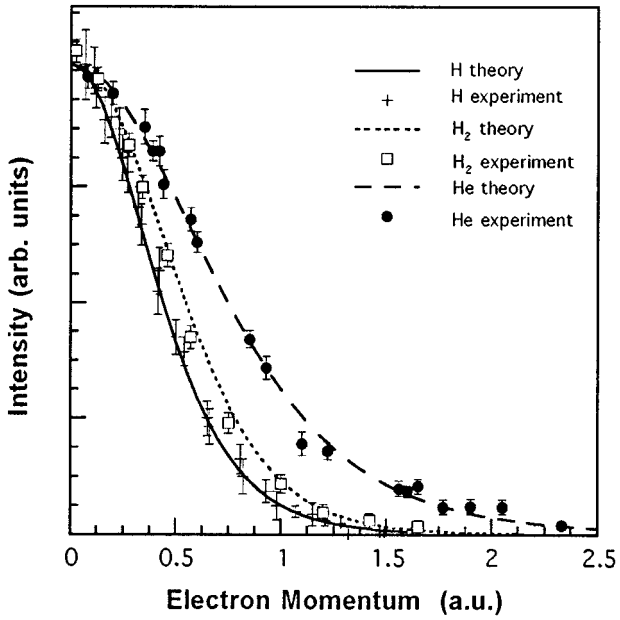

Fig. 7. Experimental momentum-density profiles for the hydrogen atom, the hydrogen molecule and the helium atom. The curves are calculated from the exact solution of the Schrödinger equation for the hydrogen atom and SCF approximations for the two-electron cases. The data are arbitrarily normalized to the same zero-momentum value.

ecule in momentum space, as well as the 1s momentum densities of hydrogen and helium atoms. Figure 6 is a contour plot of the electron density in the p_x–p_y plane, with the direction of the p_x axis being that of the internuclear axis. The three-dimensional density is symmetric under rotation about the p_x axis. In coordinate space there are centers with high electron density at each of the two nuclei. In momentum space the bonding orbital has a single center at $\mathbf{q}=0$. As is clear from Fig. 6 the momentum density of the bonding orbital is indeed between the densities for the atomic hydrogen 1s and helium 1s orbitals. The antibonding orbital is of course centered at the origin of momentum but it has two concentrations of high density away from zero. It clearly has the larger magnitude of momentum on average, i.e., it is the orbital with more kinetic energy.

The contribution of EMS to the understanding of the hydrogen-molecule bond is shown in Fig. 7, where experimental momentum densities are compared for atomic hydrogen,[10] molecular hydrogen[14] and helium.[15] Since target molecules are randomly oriented the molecular momentum density is spherically averaged. The experimental points are supplemented by calculated momentum-density curves, using SCF orbitals in the two-electron cases. The data are arbitrarily normalized to equal density at zero momentum for convenience in comparison. The expected increase in average momentum, and hence kinetic energy, in comparison with bare atoms, is observed for the hydrogen molecule. The high-momentum part of the hydrogen-molecule data is compatible with an increased effective decay constant, as expected from the promotion effect. We also observe the expected effect at low momenta. The trend of the hydrogen-molecule data is away from the hydrogen atom and towards helium.

V. MODEL FOR A SOLID

To understand the transition from a molecule to a solid we construct a hypothetical one-dimensional solid from a number of hydrogen atoms by placing them with spacing equal to that of the hydrogen molecule along a straight line. We do not know how to accomplish this in the laboratory, but still we can generate theoretical molecular orbitals. We use the SCF program for molecules GAMESS[16] with a basis of s and p functions appropriate to the hydrogen molecule, centered at the nuclei.

Since the spatial extension of the atomic-hydrogen orbitals is not small compared to the distance between the nuclei, the electrons will always experience the attractive potential from more than one nucleus. Indeed, it turns out that, if one plots the coordinate-space orbitals along the axis of the molecule for a string of 32 hydrogen atoms, they resemble the solutions of the problem of a particle in a one-dimensional box of length equal to that of the molecule [Fig. 8(a)]. They have a small modulation due to the difference between the actual potential of the 32 atoms and the smooth average potential. Only the 16 orbitals with lowest energy are occupied and plotted. We characterize them by a principal quantum number i. Along the hydrogen chain the potential of the box is lowered due to a rather uniform interaction between the electrons and the nuclei. The attractive potential of the nuclei is canceled in part by the repulsive interaction between the electrons. Let us call this average potential inside the box ϵ_0. Each solution has a characteristic wavelength λ_i. It is no surprise that the momentum-space orbital, which is the Dirac–Fourier transform [Eq. (3)] of the coordinate-space orbital, is peaked at a value q_i corresponding to the wavelength λ_i. We remind the reader that, in atomic units, wave numbers and momenta have identical numerical values. For

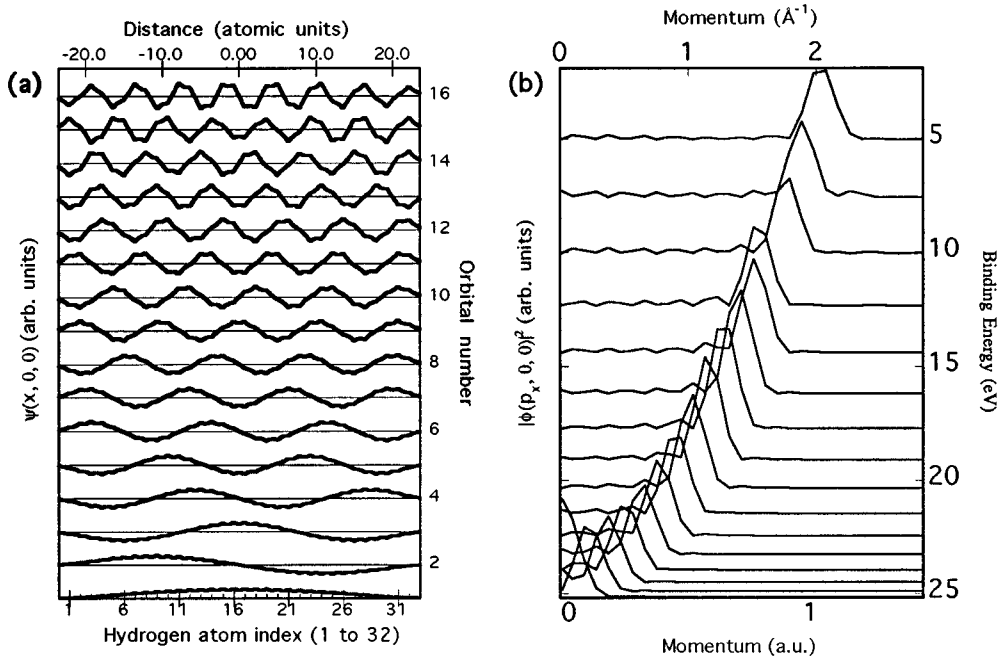

Fig. 8. (a) Shows the 16 occupied coordinate-space orbitals of a model linear H_{32} molecule. The orbitals resemble the solutions of the problem of a particle in a box. The orbital i has a characteristic wavelength λ_i of approximately $2L/i$ where L is the length of the molecule. In (b) we show the corresponding orbital momentum densities. Each has a maximum close to $2\pi/\lambda_i$. Each plot is offset vertically by an amount proportional to its binding energy. The relation between binding energy and momentum is close to the free-electron parabola.

example the least-bound orbital ($i=16$) has a wavelength of about 6 a.u. and hence its momentum distribution is expected to peak near $2\pi/6\simeq 1$ a.u.

In Fig. 8(b) we show the momentum density for each of the 16 occupied orbitals. Each curve i is shifted vertically by its calculated binding energy. The peaks at momenta q_i seem to line up along a parabola. This is not a surprise. The binding energy ϵ_i of each orbital i is the difference between the potential energy of the electron due to the interaction with the remainder of the system ϵ_0 and its kinetic energy. The kinetic energy of a free particle is $q^2/2$. Thus the binding energy of orbital i in this approximation is given by $\epsilon_i=\epsilon_0-q_i^2/2m^*$. The parameter m^* describing the shape of the parabola is the (dimensionless) effective mass. In Fig. 8(b) it is slightly (about 10%) less than the free-electron value 1.

For a string of n hydrogen atoms there would be $n/2$ occupied states, since each is occupied by two electrons of opposite spin projection. In the limit $n\to\infty$, corresponding to a one-dimensional solid, the spacing between the energy levels would become infinitesimally small and we would have a continuous dispersion relation $\epsilon=\epsilon_0-q^2/2m^*$. The continuous energy levels form an electronic band. The continuum quantity replacing the principal quantum numbers i of the discrete orbitals is a wave vector that is often called the crystal momentum, and which we denote by k to distinguish it from the real momentum q of the electron, measured by EMS.

VI. A FREE-ELECTRON METAL

In practice, we expect free-electron-like behavior, as illustrated by the model of Sec. V, for solids in which the extension of the outermost atomic orbitals is large compared to the interatomic spacing. This is the case for the elements at the left side of the periodic table. Here, new s and p levels are being filled with increasing atomic number. The electrons in these levels experience nuclear potentials that are screened to a large extent by the inner-shell electrons, and their atomic orbitals are almost as extended as the corresponding s and p orbitals for the hydrogen atom.

In Fig. 9 we show the measured energy–momentum density for an aluminum film.[17] The qualitative resemblance

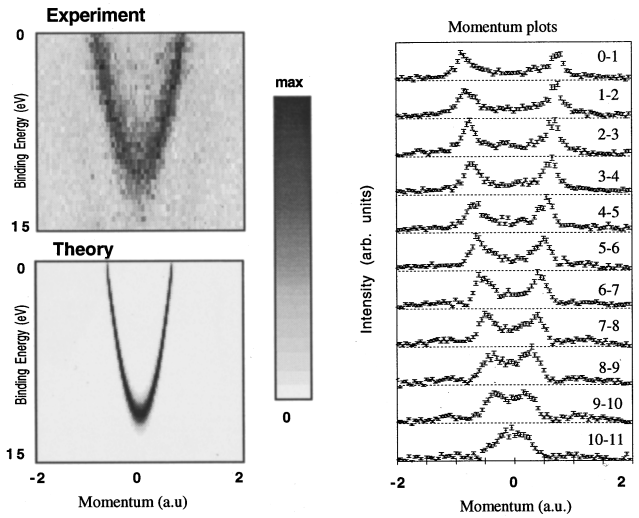

Fig. 9. The experimental results of EMS measurements for an aluminum film (top left). The parabolic shape for the binding-energy–momentum relation is indicative of a free-electron metal. At bottom left we show the results of detailed calculations of this energy–momentum density. The agreement is excellent. In the right panel we show the momentum densities for binding-energy slices indicated in eV for each plot. The resemblance to the results for the model H_{32} system is striking.

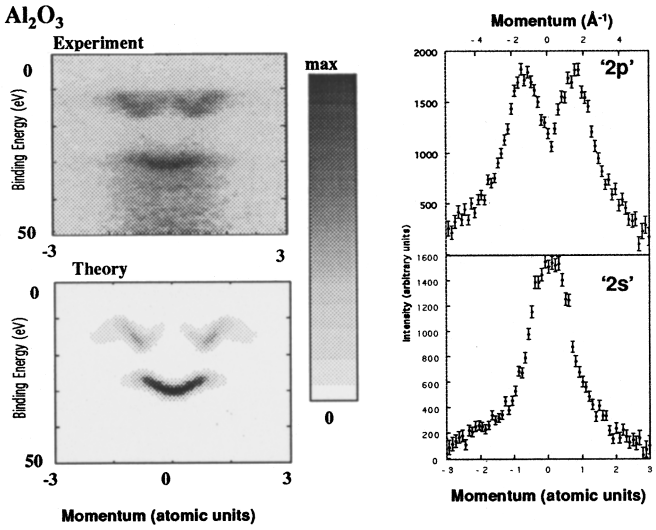

Fig. 10. The experimental results of EMS measurements on an Al_2O_3 film and the results of a corresponding calculation. The right panel shows the experimental momentum density, integrated over energy. Note that the results are completely different from those of aluminum metal. If anything they more closely resemble the argon gas data of Fig. 4.

with the calculated shape for the chain of hydrogen atoms is striking. The outer valence electrons in aluminum are essentially free. They behave as in the model of a particle in a box, with the dimensions of the box being equal to the dimensions of the solid sample. In Fig. 9 we also show the results of quantum-mechanical calculations using state-of-the-art computer codes.[17] There is good agreement, both for the energy–momentum (dispersion) relation and the corresponding electron density. The main difference is that there is more contrast in the theoretical plots. This is because in the experiment some of the external electrons have suffered additional elastic collisions, causing slight broadening of the momentum peak for each energy, and thus decreasing the contrast.

VII. AN IONIC SOLID

That a free-electron type of behavior is not typical for all solids becomes clear if we expose the aluminum film to air. The film will oxidize near the surface. Due to the small mean free path of the slow external electron in the EMS reaction we obtain information only from the surface of the thin film nearest the detectors. Therefore the image obtained from this film shows only the oxidized layer. This image is shown in Fig. 10.[18] It has no resemblance to the aluminum metal at all; rather, it resembles the atomic-argon picture.

What is the explanation for this? Aluminum oxide has the composition Al_2O_3. In the simple ionic picture we have Al^{3+} and O^{2-}. Both of them have the first two shells completely filled, so that their electronic structure resembles that of the noble gas neon. The binding energies of the $2s$ and $2p$ electrons in Al^{3+} will be greater than those for O^{2-}, since the oxygen nucleus has a smaller charge. Therefore the outermost orbitals of Al_2O_3 are the $2p$ and $2s$ orbitals associated with the oxygen atoms. All occupied orbitals are much smaller than the (now unoccupied) Al $3s$ and Al $3p$ orbitals. So the free-electron picture, valid for metallic aluminum, does not apply to Al_2O_3. The image for the oxide is more like the pure ionic picture, in which the solid is kept together by the electrostatic attraction of two relatively inert, oppositely charged ions and the electrons are mainly associated with an orbital of one ion only.

That the free-ion picture is too simple is clear from a somewhat-more-careful inspection of Fig. 10. Both the deeper ''s'' density and the ''p'' density are not associated with a constant energy level as in the case of a noble gas, but there is dependence of the binding energy on the momentum (i.e., dispersion). The maximum binding energy of the inner $2s$ level is at zero momentum. However, the p level has its maximum binding energy at a finite momentum. This can be interpreted in a straightforward manner using a chain of hydrogen atoms similar to that introduced in Sec. V.

In ionic solids the overlap between orbitals centered at different nuclei is small. In the linear-chain model, the hydrogen atoms are now separated by a much larger distance than in a hydrogen molecule. We consider both a chain of hydrogen atoms with occupied $1s$ orbitals (mimicking the s level in Al_2O_3) and one where the $2p$ orbitals are occupied (mimicking the p level of Al_2O_3).

In Fig. 11(a) we show a chain of 11 hydrogen $1s$ orbitals. The spacing a of the atoms is chosen to be 2.5 Å in this case, so there is only small overlap between neighboring atomic orbitals. For these s electrons we can construct the lowest bonding orbital if we add all atomic orbitals with the same phase. This is shown by the thin line of Fig. 11(b). It is energetically most favorable since the interference between the nuclei is constructive. If we construct an antisymmetric orbital by changing the sign of the atomic orbital at alternate atoms, we get the antibonding orbital. It is energetically less favorable as it has destructive interference between the nuclei. Again the momentum-space orbital will peak at momenta corresponding to the characteristic wavelength of the coordinate-space orbital. At zero momentum the Dirac–Fourier transformation averages the orbital over all space. The bonding orbital has a large constant component and hence its momentum distribution will peak at zero momentum. The antibonding orbital averages to zero at zero momentum. Its wavelength is $2a$ and thus its Dirac–Fourier transform will peak at $q=2\pi/2a$.

For the case of hydrogen atoms with the $2p$ orbital occupied we choose the distance a between neighboring atoms larger (10 Å) in order to have small overlap of the orbitals of adjacent atoms [Fig. 11(c)]. Again we construct symmetric and antisymmetric sums of these orbitals [Fig. 11(d)] but there are some differences from the s-derived orbitals. The symmetric sum (thin line) and antisymmetric sum (thick line) of the p orbitals both average to zero, i.e., they have zero density for zero momentum. Now the antisymmetric sum oscillates with the longer wavelength ($2a$) and its momentum density peaks near $2\pi/2a$. It is the orbital with enhanced charge density between the atoms, i.e., the bonding orbital (see also Fig. 5). The symmetric sum has a shorter wavelength (a) and hence its momentum density will peak around $2\pi/a$. It has a node between the nuclei, so it is the antibonding orbital. Different combinations occur at different momenta from these two extremes and their binding energies are between the extreme values. Hence there is an energy minimum at momentum $2\pi/2a$.

What does this mean for Al_2O_3? The crystal structure of Al_2O_3 is very complicated. It even exists in three different forms, α-, γ-, or η-alumina. In the α-alumina form the minimum distance between oxygen atoms is about 4.7 a.u. (2.5 Å). For the s level we find maximum binding energy as

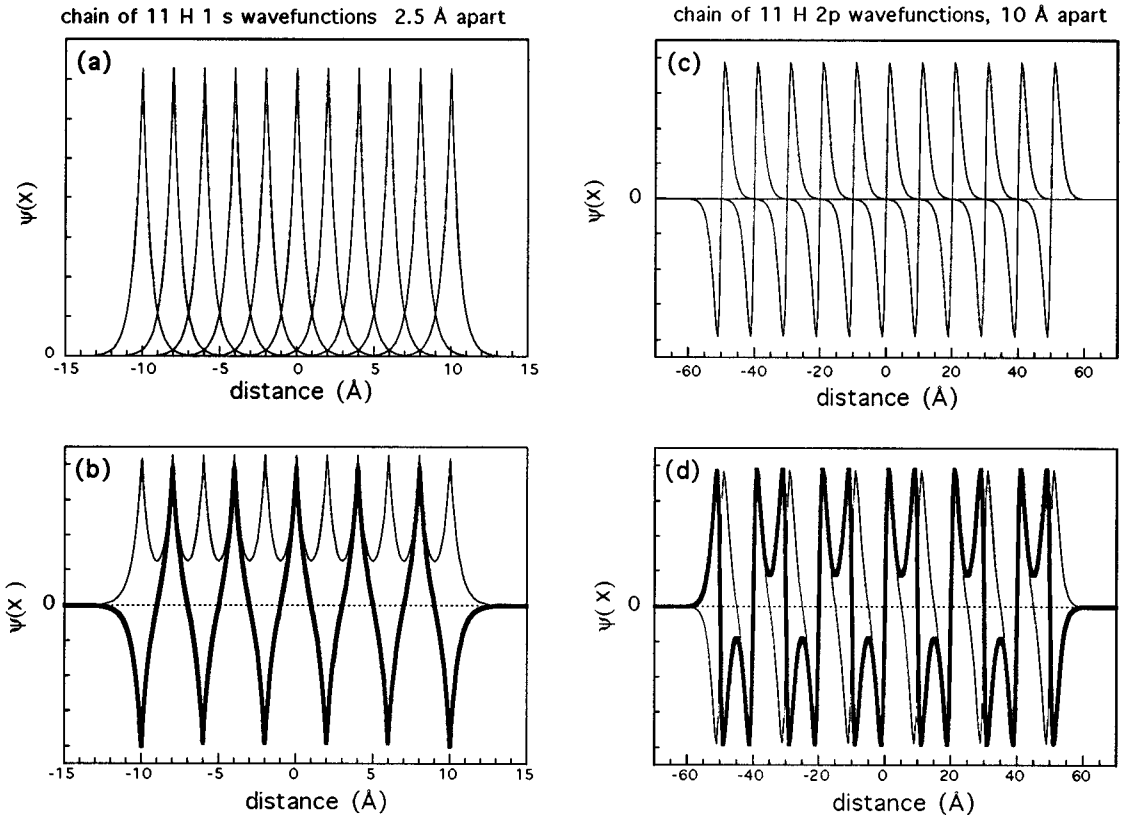

Fig. 11. Examples of different molecular orbitals constructed from atomic orbitals separated by a distance a. In (a) we have 11 hydrogen 1s orbitals and we have chosen $a=2.5$ Å, so that the atomic orbitals have small but significant overlap. In (b) we show the symmetric (thin line) and antisymmetric (thick line) linear combinations. The symmetric combination has larger interference density and is therefore the bonding orbital. In (c) we have 11 hydrogen 2p wave functions. In order to have again small but significant overlap we take $a=10$ Å. Now the symmetric sum (thin line) has smaller interference density than the antisymmetric sum (thick line). Each molecular orbital has a characteristic repeating distance (wavelength) L, which can be read from the figure. The corresponding momentum distribution peaks at $2\pi/L$ as explained in the text.

expected at zero momentum and we reach the top of the band at about 0.75 a.u., in fair agreement with the prediction of our model ($2\pi/2a=0.67$ a.u.) For the p-derived band our model predicts maximum binding energy for this momentum value, as is indeed the case in the experiment. The minimum binding energy for the p-derived band is found experimentally near 1.3 a.u., again in good agreement with the prediction of our model ($2\pi/a=1.34$ a.u.).

VIII. CONCLUSION

We have shown how EMS observes electronic structure very directly and in sufficient detail to confirm experimentally our understanding of the chemical bond. By extending the theoretical description of molecular bonding we have developed a simple understanding of the electronic band structure of solids. Explanations similar to some of ours are common in textbooks on solid-state physics and are illustrated by simple calculations. For the first time it is possible to illustrate them by experiments that directly measure energy–momentum densities.

We have described the transition from atom to molecule to solid by an interplay of experiment and theory. The momentum discrimination, in addition to the common spectroscopic energy discrimination, makes EMS the most powerful tool for this purpose.

ACKNOWLEDGMENTS

The authors want to thank all their co-workers of the Electronic Structure of Materials Centre for the use of partly unpublished material and for many stimulating discussions. We also thank Professor Wolf Weyrich for very useful discussions and suggestions. The research was funded by a grant of the Australian Research Council.

[a]Present address: Research School of Physical Sciences and Engineering, Australian National University, Canberra 0200, Australia.

[1]I. E. McCarthy and E. Weigold, ''Electron momentum spectroscopy of atoms and molecules,'' Rep. Prog. Phys. **54**, 789–879 (1991).
[2]J. W. M. DuMond, ''The linear momenta of electrons in atoms and in solid bodies as revealed by x-ray scattering,'' Rev. Mod. Phys. **5**, 1–33 (1933).
[3]M. J. Cooper, ''Compton scattering and electron momentum determination,'' Rep. Prog. Phys. **48**, 415–481 (1985).
[4]R. Courths and S. Hüfner, ''Photoemission experiments on copper,'' Phys. Rep. **112**, 53–171 (1984).
[5]M. Vos and I. E. McCarthy, ''Observing electron motion in solids,'' Rev. Mod. Phys. **67**, 713–723 (1995).
[6]J. R. Dennison and A. L. Ritter, ''Application of (e,2e) spectroscopy to the electronic structure of valence electrons in crystalline and amorphous solids,'' J. Electron. Spectrosc. Relat. Phenom. **77**, 99–142 (1996).
[7]Y. Zheng, J. J. Neville, and C. E. Brion, ''Imaging the electron density in the highest occupied orbital of glycine,'' Science **270**, 786–788 (1995).
[8]R. Camilloni, A. Giardini-Guidoni, R. Tiribelli, and G. Stefani, ''Coincidence measurements of quasifree scattering of 9 keV electrons of K and L shells of carbon,'' Phys. Rev. Lett. **29**, 618–621 (1972).

[9]P. Storer, S. A. C. Clark, R. C. Caprari, M. Vos, and E. Weigold, ''Condensed matter electron momentum spectrometer with parallel detection in energy and momentum,'' Rev. Sci. Instrum. **65**, 2214–2226 (1994).
[10]B. Lohmann and E. Weigold, ''Direct measurement of the electron momentum probability distribution in atomic hydrogen,'' Phys. Lett. A **86**, 139–141 (1981).
[11]I. E. McCarthy and E. Weigold, ''A real 'thought' experiment for the hydrogen atom,'' Am. J. Phys. **51**, 152–155 (1983).
[12]C. A. Coulson, ''Gamma-ray Compton profiles of diamond, silicon and germanium,'' Proc. Cambridge Philos. Soc. **37**, 55–66 (1941).
[13]K. Ruedenberg, ''The physical nature of the chemical bond,'' Rev. Mod. Phys. **34**, 326–376 (1962).
[14]S. Dey, I. E. McCarthy, P. J. O. Teubner, and E. Weigold, ''(e,2e) probe for the hydrogen-molecule wave function,'' Phys. Rev. Lett. **34**, 782–785 (1975).
[15]I. E. McCarthy and E. Weigold, ''(e,2e) spectroscopy,'' Phys. Rep. **27**C, 275–371 (1976).
[16]M. W. Schmidt, J. A. Boatz, K. K. Baldridge, S. Koseki, M. S. Gordon, S. T. Elbert, and B. Lam, ''GAMESS User's Guide,'' QCPE Bull. **7**, 115–140 (1987).
[17]S. A. Canney, M. Vos, A. S. Kheifets, N. Clisby, I. E. McCarthy, and E. Weigold, ''Measured energy–momentum densities of the valence band of aluminum,'' J. Phys: Condens. Matter **9**, 1931–1950 (1997).
[18]X. Guo, S. Canney, A. S. Kheifets, M. Vos, Z. Fang, S. Utteridge, I. E. McCarthy, and E. Weigold, ''Electronic structure investigation of oxidized aluminum films with electron momentum spectroscopy,'' Phys. Rev. B **54**, 17943–17953 (1996).